Carbohydrate Polymers 90 (2012) 322–332

Contents lists available at SciVerse ScienceDirect

Carbohydrate Polymers

journal homepage: www.elsevier.com/locate/carbpol

Structure of arabinogalactan-protein from Acacia gum: From porous ellipsoids to supramolecular architectures

D. Renard[a,*], C. Garnier[b], A. Lapp[c], C. Schmitt[d], C. Sanchez[e]

[a] INRA, UR1268 Biopolymères Interactions Assemblages, F-44300 Nantes, France
[b] UMR CNRS 6290 Equipe TAF «Translation and Folding», Université de Rennes 1, Campus Beaulieu, F-35042 Rennes Cedex, France
[c] Laboratoire Léon Brillouin, CEA Saclay, Bâtiment 563, F-91191 Gif-sur-Yvette, France
[d] Department of Food Science and Technology, Nestlé Research Center, Vers-chez-les-Blanc, CH-1000 Lausanne 26, Switzerland
[e] UMR1208 Ingénierie des Agropolymères et Technologies Emergentes, INRA-Montpellier SupAgro-CIRAD-Université Montpellier 2, Place Pierre Viala, F-34060 Montpellier, France

ARTICLE INFO

Article history:
Received 22 March 2012
Received in revised form 14 May 2012
Accepted 16 May 2012
Available online 26 May 2012

Keywords:
HPSEC-MALLS
Small-angle neutron scattering
Transmission electron microscopy
Arabinogalactan-protein
Supramolecular assemblies
Acacia gum

ABSTRACT

The structure of the arabinogalactan-protein (AGP) fraction of the gum exudate of *Acacia senegal* (gum Arabic) isolated from hydrophobic interaction chromatography was investigated using HPSEC-MALLS, small angle neutron scattering and TEM observations. Literature reported that the AGP structure of gum Arabic adopts a very compact conformation in solution due to the attachment of short arabinoside side chains and much larger blocks of carbohydrate to the polypeptidic backbone. The present study revealed that AGP in solution had a weight average molecular weight M_w of 1.86×10^6 g mol^{-1} and a radius of gyration R_g of 30 nm. In addition, two exponent values were identified in the R_g, $[\eta]$, R_h and ρ vs. M_w relationships highlighting two types of conformations depending on the molecular weight range considered: a low molar mass population with long-chain branching and a compact conformation and a high molar mass population with short-chain branching and an elongated conformation. AGP would behave in solution as a branched or hyper-branched polymer with conformations ranging from globular to elongated shape depending on the size of the carbohydrate branches. Small angle scattering form factor revealed an elongated average conformation corresponding to a triaxial ellipsoid while inverse Fourier transform of the scattering form factor gave a maximum dimension for AGP of 64 nm. Transmission electron microscopy highlighted the existence of two types of flat objects with thicknesses below 3–5 nm, single particles with a more or less anisotropic spheroidal shape and aggregated structures with a more elongated shape. A remarkable feature of all particle morphologies was the presence of an outer structure combined to an inner more or less porous network of interspersed chains or interacting structural blocks, as previously found for the arabinogalactan (AG) main molecular fraction of Acacia gum. However, clear differences were observed in the density and morphology of the inner porous network, probably highlighting differences in the degree of branching. The existence of assembled AG as part of the AGP family was confirmed using TEM micrographs at high resolution. Fused AGP dimers, trimers, tetramers and multimers were also identified. These molecular assemblies questioned about the nature of interactions involved.

1. Introduction

Acacia gum, or gum Arabic, is the oldest and best known of all natural gums. It was widely used by the ancient Egyptians (5000–3000 B.C.), however its use as food traced back in the Stone Age (Chevalier, 1924). Although Acacia gum has also been used as an adhesive in modern times, the most important applications are in food, pharmaceutical, cosmetic, and lithography industries (Majewska-Sawka & Nothnagel, 2000). In particular, Acacia gum is considered the premier oil-in-water emulsifier and is used to encapsulate flavour in the manufacture of bakery products, beverages, and desserts (Pettolino, Liao, Ying, Mau, & Bacic, 2006).

Acacia gum is a branched, neutral or slightly acidic, complex polysaccharide obtained as a mixed calcium, magnesium and potassium salt. The main chain consists of 1,3-linked β-D-galactopyranosyl units. The side chains are composed of two to five 1,3-linked β-D-galactopyranosyl units, joined to the main chain by 1,6-linkages. Both the main and the side chains contain units of α-L-arabinofuranosyl, α-L-rhamnopyranosyl, β-D-glucuronopyranosyl, and 4-O-methyl-β-D-glucuronopyranosyl, the latter two mostly as end-units (Anderson & Stoddart, 1966). Acacia gum would be composed by 64 ramified 1,3-linked homogalactan symmetrically arranged sub-units, each of molecular mass 8000 g mol^{-1} (Churms, Merrifield, & Stephen, 1983).

* Corresponding author. Tel.: +33 2 40 67 50 52; fax: +33 2 40 67 50 25.
E-mail address: drenard@nantes.inra.fr (D. Renard).

0144-8617/$ – see front matter © 2012 Elsevier Ltd. All rights reserved.
http://dx.doi.org/10.1016/j.carbpol.2012.05.046

Acacia gum contains about 2% of a polypeptide (Anderson, Bridgeman, Farquhar, & McNab, 1983). It is a highly heterogeneous material, because it has, on the one hand, a variation in monomer composition and/or in the linking and branching of the monomer units and, on the other hand, a molecular mass distribution. The consequence of this heterogeneity is reflected through the molecular species collected after fractionation of Acacia gum and the mode of both separation and detection used. In general, three main fractions can be isolated by hydrophobic interaction chromatography (Randall, Phillips, & Williams, 1989). Analysis of the fractions showed that each contained similar proportions of the various sugars and differed essentially in their molecular masses and protein contents. The bulk of the gum (88.4 wt% of the total) was shown to be comprised by an AG fraction with a weight-average molecular weight $\overline{M}_w$ of 2.86×10^5 g mol^{-1} and a low protein content (0.35 wt%). The second major fraction (10.4 wt% of the total) was identified as an AGP with a molecular weight of 1.86×10^6 g mol^{-1} and contained a greater proportion of protein (11.8 wt%). The third minor fraction (1.2 wt%) will consist of one, or possibly two, glycoproteins (GP). One of the GP had a molecular weight of 2.5×10^5 g mol^{-1} and the highest protein content (47.3 wt%) (Renard, Lavenant-Gourgeon, Ralet, & Sanchez, 2006). The proteinaceous component of the first two fractions had similar amino acid distributions, with hydroxyproline and serine being the most abundant. The amino acid composition of the third fraction was significantly different with aspartic acid being the most abundant (Renard et al., 2006). Since the three main fractions are precipitated by the Yariv reagent, they can be classified as AGP type macromolecule.

The AG fraction was identified by so far as the main fraction and would consequently play a key role in the functional properties of the whole gum. Previous work performed in the laboratory aimed to characterize both structural and rheological properties of Acacia gum dispersions (Sanchez, Renard, Robert, Schmitt, & Lefebvre, 2002). From HPSEC-MALLS measurements and rheology, it was tentatively suggested that Acacia gum molecules displayed a random coil shape with some unusual rheological behaviour ascribed to interplay between surface and bulk rheological properties of Acacia gum dispersions. We recently showed that AG from Acacia gum was an oblate ellipsoid with ~20 nm diameter and ~1.5 nm thickness with an inner interspersed chains network (Sanchez et al., 2008). The model proposed was a real breakthrough in the field of arabinogalactan-protein-type macromolecules.

The tertiary structure of the arabinogalactan-protein (AGP) molecular fraction has been described in terms of a wattle-blossom macromolecular assembly by virtue of which few (~5) discrete polysaccharide domains of $\overline{M}_w \sim 2 \times 10^5$ g mol^{-1} are held together by a short peptide backbone chain (Fincher, Stone, & Clarke, 1983). More recently, Mahendran et al. identified smaller carbohydrate blocks of $\sim 4.5 \times 10^4$ g mol^{-1} linked by *O*-serine and *O*-hydroxyproline residues to the polypeptide chain of approximately 250 amino acids in length (Mahendran, Williams, Phillips, Al-Assaf, & Baldwin, 2008). The key experimental evidences to support this hypothesis showed that hydrolysis of the AGP fraction with a protease or different chemical treatments produced, respectively, a five and forty four-fold reduction in molecular weight. The authors therefore proposed a new model where the shape of the macromolecule would be a kind of spheroidal random coil consistent with the wattle-blossom structure. This spheroidal random coil would be composed of a folded polypeptide chain carrying large sugar blocks with a possible thin oblate ellipsoid morphology (Mahendran et al., 2008). The model is interesting since it gives a clearer picture of the possible spatial configuration of AGP. However, the steric arrangement of carbohydrate blocks in such a configuration is unclear as well as the possible interactions between carbohydrate blocks.

An alternative model was proposed which described the Acacia gum glycoprotein as a statistical model with a fundamental 7×10^3 g mol^{-1} subunit, where polysaccharide side chains attach to a polypeptide backbone of probably more than 400 residues in a highly regular and ordered fashion (every 10–12 residues repetitive peptide units), forming a 'twisted hairy rope' of ~150 nm long, 5 nm diameter and an axial ratio of ~30:1 (Qi, Fong, & Lamport, 1991). This model would be consistent with the fact that large macromolecules, like AGPs, could migrate through a primary cell wall with a 4–5 nm porosity by reptation (Carpita, 1982).

The objectives of the present study was to gain further insight into the structure of the AGP fraction in order to decipher between the wattle-blossom and twisted hairy rope models or alternatively to propose a new model by applying small angle neutron scattering and microscopic methods. A better knowledge of the structure of the arabinogalactan-protein fraction from gum Arabic should improve the understanding of both biological and technological function of this important class of macromolecules.

2. Materials and methods

2.1. Materials

Spray-dried Acacia gum (lot 97J716) from *Acacia senegal* trees was a gift from CNI Company (Rouen, France). Before purification, Acacia gum was extensively dialysed against deionized water and freeze-dried. All chemicals were of analytical grade and were obtained from Merck, Sigma and Aldrich.

2.2. Purification of AGP molecular fraction

The arabinogalactan-protein (AGP) molecular fraction of Acacia gum was purified by Hydrophobic Interaction Chromatography as described previously (Renard et al., 2006). Purified AGP was dialysed then freeze-dried before further characterization.

2.3. Preparation of AGP dispersions

Known amounts of AGP powder previously dialysed and freeze-dried were dispersed in the appropriate solvent conditions (50 mM NaCl or $NaNO_3$) one night at room temperature under gentle stirring conditions. The dispersions were centrifuged 40 min at $16{,}000 \times g$ to remove air bubbles and undissolved material. The centrifuged AGP dispersions were then filtered through 0.2 μm Anotop membranes (Anotop, Alltech, France) for light and neutron scattering experiments.

2.4. High-performance size exclusion chromatography-multi angle laser light scattering (HPSEC-MALLS)

The determination of molecular weight and size distributions of AGP was performed by coupling on line to a high-performance size exclusion chromatography, a multi-angle laser light scattering detector, a differential refractometer and a differential viscosimeter. AGP dispersions at 0.04 wt% into 50 mM $NaNO_3$ buffer containing 0.02% NaN_3 as preservative were filtered through 0.2 μm Anotop membranes (Anotop, Alltech, France), and injected on a HPSEC system constituted of a Shodex OH SB-G precolumn followed by two Shodex OH-pack 804 HQ and 805 HQ columns used in series. The samples were eluted at 0.7 mL min^{-1} with a 50 mM $NaNO_3$ solution. On-line molecular weight and intrinsic viscosity determinations were performed at room temperature using a multi-angle laser light scattering (MALLS) detector (mini-Dawn, Wyatt, Santa Barbara, CA, operating at three angles: 41°, 90° and 138°), a differential refractometer (ERC 7547 A)

($dn/dc = 0.171\ mL\ g^{-1}$), and a differential viscosimeter (T-50A, Viscotek). Weight (M_w) and number (M_n) average molecular weights ($g\ mol^{-1}$) and radius of gyration (R_g, nm) were calculated using Astra 1.4 software (Wyatt). Intrinsic viscosity [η] was calculated using TriSEC software, version 3.0 (Viscotek).

2.5. Static and dynamic light scattering

Light scattering experiments on filtrated AGP ($C = 1$ wt%) dissolved in 50 mM $NaNO_3$ solution were performed at $T = 25\ ^\circ C$ ($\pm 0.1\ ^\circ C$) using an ALV-5000 multi-bit, multi-tau correlator in combination with a Malvern goniometer and a Spectra-Physics laser emitting vertically polarized light at 514.5 nm.

Static light scattering (SLS) experiments on AGP sample and its corresponding solvent were done between $\theta = 30^\circ$ and 150°, θ being the scattering angle, toluene being used as the reference. After normalization of the scattered intensity by the solvent and the toluene at all scattering angles, the Guinier approximation, Ln I vs. q^2, with the wave vector $q = 4\pi n/\lambda \sin(\theta/2)$, was used to determine the AGP radius of gyration R_g.

The correlation functions obtained by dynamic light scattering (DLS) at $\theta = 30^\circ$, 90° and 150° scattering angle were analysed using the inverse Laplace transform routine REPES (Štepánek, 1993) in order to obtain the corresponding relaxation time distribution (and hydrodynamic radii distribution).

Only one population with a radius of gyration (R_g) and a hydrodynamic radius (R_h) of 30 and 34.4 nm, respectively, were determined for AGP in solution.

2.6. Small angle neutron scattering (SANS) experiments and data treatment

SANS experiments and data treatment were performed as described previously (Sanchez et al., 2008). Briefly, scattering experiments on filtrated AGP ($C = 1$ wt%) dissolved in 50 mM NaCl solution in 99.8% D_2O in order to get the form factor $P(q)$ were performed on the D22 instrument at the ILL (Grenoble, France) using a spectrometer configuration $\lambda = 8$ Å (incident wavelength), $d = 8$ m (distance of the sample to the detector). The range of the wavevector $q = 4\pi/\lambda \sin(\theta/2)$, θ being the scattering angle, thus covered was: 4.65×10^{-2}–$2.86\ nm^{-1}$. The data were normalized for transmission and sample path length and divided by the water spectrum. An absolute intensity scale was obtained using the absolute value of water intensity in units of cross-section (cm^{-1}). A subtraction of the appropriate incoherent background, taking H/D exchange on AGP into account, was realized. Experiments were carried out at different AGP concentrations (1, 2, 5 or 10 wt%) and at 1 wt% AGP concentration in D_2O containing different NaCl concentrations (5, 10, 20, 50, 100 and 500 mM). The form factor $P(q)$ of AGP was obtained at 50 mM NaCl concentration where intermolecular interactions were negligible and therefore $S(q) = 1$.

The pair distance distribution function $P(r)$ together with the structural parameter derived from $P(r)$, i.e. the maximum dimension of the particle (D_{max}) was computed from the form factor by the indirect Fourier transform program GNOM (Svergun, 1992; Svergun, Semenyuk, & Feigin, 1988). Fit of experimental AGP form factor by different theoretical form factors was assayed using the SansView software v2.0.1 (http://danse.chem.utk.edu/sansview.html).

2.7. Transmission electron microscopy (TEM) and image analysis

AGP samples were prepared in the same conditions as those reported in Sanchez et al. (2008) for microscopy observations. For TEM, 4 μL AGP samples (0.01–0.1 wt%) were applied on carbon-coated copper grids (300 mesh), and allowed to stand for 30–120 s. The grids were then rinsed with ammonium acetate and negatively stained for 30 s with 2% (w/v) uranyl acetate, and wicked dry prior to analysis using a CM12 Philips transmission electron microscope operating at accelerating voltages of 120 kV. Pictures obtained from TEM were treated using the ImageJ freeware v1.45o. Generally the treatment consisted in capturing one object, changing the image contrast and filtering using a bandpass FFT filter. Sometimes an additional filtering was made using the CLAE (Contrast Limited Adaptive Histogram Equalization) ImageJ plugin that enhances the local contrast of images. After filtering, 3D rendering was applied through the Interactive 3D Surface Plot v2.33 plugin. Pictures ($n = 25$) were also treated to extract distribution of structural dimensions of objects. In this case, image contrast was modified, then thresholding was made to obtain binary images. Structural dimensions of objects were then computed using ImageJ.

3. Results

3.1. HPSEC-MALLS measurements

Previous data performed using HPSEC-MALLS identified an asymmetric distribution of AGP from Acacia gum (Fig. 1a) with a weight average molecular weight (M_w) of $1.86 \times 10^6\ g\ mol^{-1}$, a radius of gyration R_g of 30 nm, a polydispersity index (M_w/M_n) of 1.33 and an intrinsic viscosity [η] value of $70.7\ mL\ g^{-1}$ (Renard et al., 2006). It was interesting to notice that the R_g values determined using static light scattering at fixed AGP concentration (1 wt%) or using HPSEC-MALLS at AGP infinite dilution were identical, highlighting the remarkable stability of AGP at concentrations smaller or equal to 1 wt%.

For samples with a sufficiently high molecular weight, dimensions extrapolated to the infinite dilution depend on the molecular weight (at a constant temperature) as a simple power law for monodisperse polymers according to:

$$R_g = K_G M_w^{\nu} g \quad (1)$$

$$R_h = K_h M_w^{\nu} h \quad (2)$$

$$[\eta] = K_\alpha M_w^{\alpha} \quad (3)$$

where R_g, R_h, [η] and M_w are the z-average radius of gyration, the z-average hydrodynamic radius, the z-average intrinsic viscosity and the weight average molecular weight, respectively; ν_g, ν_h and α are the corresponding hydrodynamic coefficients; and K_G, K_h and K_α are the corresponding constants. The exponents remain universal in the context of these laws. The values of ν_g, ν_h and α are dependent upon polymer shape, temperature, and polymer-solvent interactions: $\nu_g = \nu_h = 0.33$, $\alpha = 0.3$ for a sphere, $\nu_g = \nu_h = 0.5$–0.6, $\alpha = 0.5$–0.8 for a linear random coil and $\nu_g = \nu_h = 1$, $\alpha = 1.8$ for a rod (Table 1) (Burchard, 1999). The pre-factors, which are constant, are non-universal: they depend on the detailed monomer structure and on the solvent chosen. The relationships between R_g, [η], R_h vs. M_w were thus analysed taking into account the best signal to noise ratio of light scattering detector, i.e. size distribution ranging from $M_w \sim 1 \times 10^6\ g\ mol^{-1}$ to $M_w \sim 4 \times 10^6\ g\ mol^{-1}$ and corresponding to 80% of the total weight distribution (Fig. 1b–d). The log–log plot of R_g vs. M_w (Fig. 1b) exhibited two slopes with exponent values ν_g of 0.41 in the $\sim$1–$2.1 \times 10^6\ g\ mol^{-1}$ M_w range and 0.91 in the $\sim$2.1–$4 \times 10^6\ g\ mol^{-1}$ M_w range. The appearance of two experimental exponent values would mean in first approximation that AGP would adopt two types of conformations depending on the M_w distribution, a shape between a hard sphere and random coil for the low M_w range and a more extended shape for the high M_w. These two possible conformations could be due to different morphologies or similar morphologies but different affinities for the solvent.

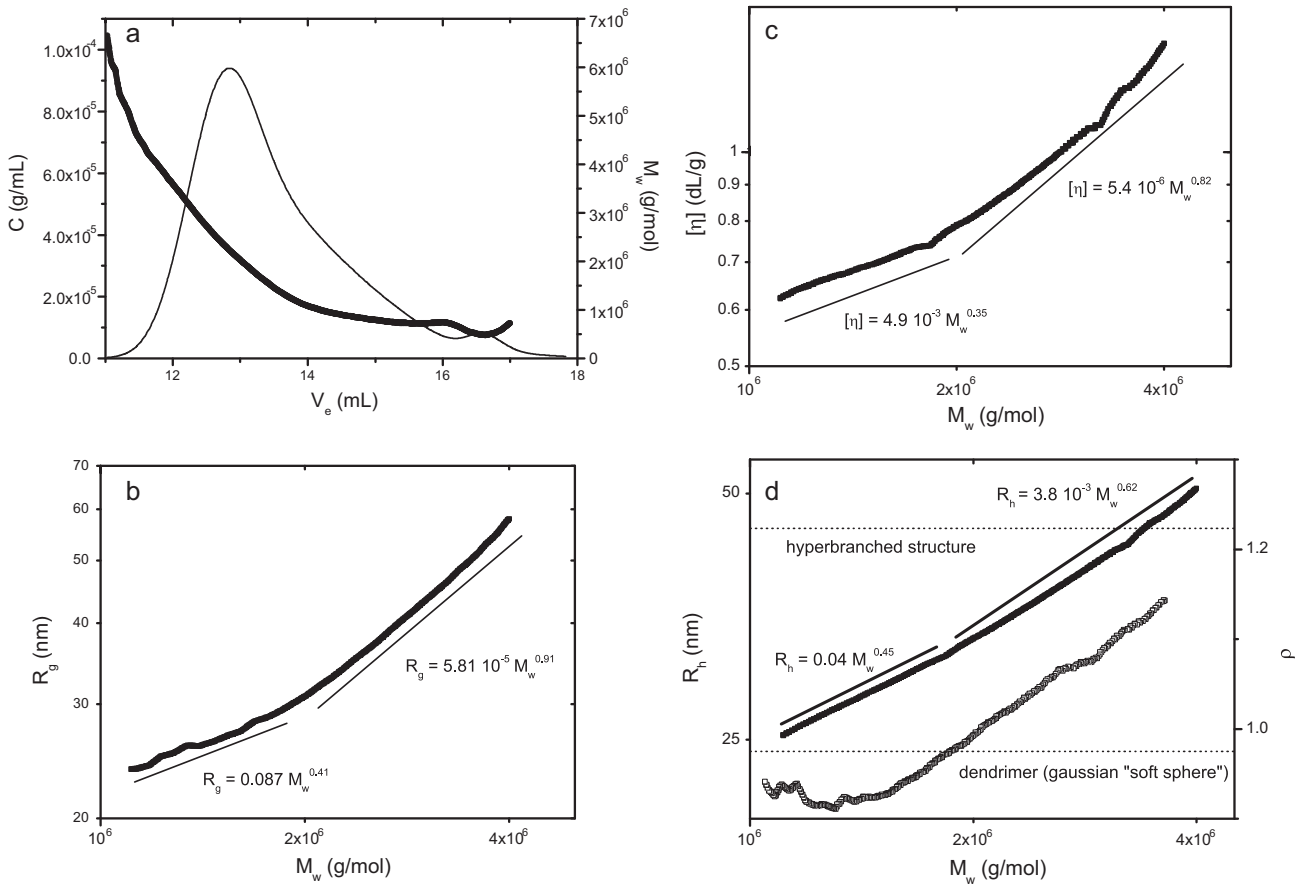

Fig. 1. (a) High performance size exclusion chromatography (HPSEC) chromatogram showing the elution profile monitored by refractive index (C, g/mL) and light scattering (M_w, g mol^{-1}) for arabinogalactan-protein (AGP) from Acacia gum, (b) radius of gyration (R_g, nm), (c) intrinsic viscosity ([η], dL/g) and (d) hydrodynamic radius (R_h nm) and structure factor ρ as a function of molecular weight (M_w, g mol^{-1}) obtained from HPSEC coupled to on-line viscosimeter and multi-angle light scattering (MALLS) detector; R_h was calculated from [η] results displayed in (c).

Further analyses using the Mark-Houwink-Sakurada (MHS) relationship [η] vs. M_w should help in deeper defining the conformation of AGP with increasing molecular weight as exponent values in this latter case would also reflect quality of the solvent. The log–log plot of [η] vs. M_w (Fig. 1c) displayed also two slopes with α exponent values of 0.35 and 0.82 with increasing molecular weight M_w. These experimental α exponent values would be partly in agreement with random coils conformations in theta or good solvent conditions as theoretical values of 0.5 and 0.8 for flexible chains in theta and good solvents (excluded volume limit), respectively, were reported (Table 1) (Ross-Murphy, 1994). The pre-factor in the [η] vs. M_w relationship is in part related to the solvent polarity (Shen, Mu, Yu, & Chen, 2004) and for flexible chains it typically ranges from 10^{-6} to 10^{-4} mL g^{-1} (Kawahigashi, Sumida, & Yamamoto, 2005). K values of 4.9×10^{-3} and 5.4×10^{-6} were obtained from linear fitting. The pre-factor and exponent values obtained from the [η] = $f(M_w)$ relationship indicated that AGPs adopted a flexible chain conformation and that water was a moderately good solvent in particular for the low M_w range of AGP. An exponent value of 0.47 was reported for total Acacia gum (Idris, Williams, & Phillips, 1998), the authors indicating that such a value would be indicative of a compact globular structure.

Using M_w and [η], we calculated the hydrodynamic radius (R_h) of AGP, assuming a spherical shape, following the equation $R_h = (3M_w[\eta]/10\pi N_a)^{1/3}$ (Tanford, 1961), with N_a the Avogadro's number. A linear relationship between R_h and M_w was found on a

Table 1
Exponent (ν_g, α and ν_h) values determined from $R_g = f(M_w)$, [η] = $f(M_w)$ and $R_h = f(M_w)$ relationships, respectively, established from HPSEC-MALLS measurements for the arabinogalactan-protein (AGP) from Acacia gum. The structure-sensitive ρ-parameter ($\rho = R_g/R_h$), determined by HPSEC-MALLS[1] and SLS and DLS[2] were also reported. Theoretical exponent, structure-sensitive ρ-parameter for different conformations were also given for comparison.

Exponent	Theory					Experiment
	Sphere	Dendrimer (Gaussian soft sphere)	Hyperbranched polymer	Linear random coil	Rod	
ν_g	0.33			0.5–0.6	1	0.41 0.91
α	0			0.5–0.8	2	0.35 0.82
ν_h	0.33			0.5–0.6	1	0.45 0.62
ρ	0.778	0.977	1.225	1.504–1.780		0.93–1.14[1] 0.87[2]

log–log plot representation (Fig. 1d) with two exponent values ν_h of 0.45 and 0.62 with increasing molecular weight M_w, these two values being in agreement with a random coil in θ (0.50) or good (0.60) solvent conditions (Table 1) (Burchard, 1994). These two exponent values would also mean that water would be a good solvent for the AGP of higher M_w and a moderate good solvent for the AGP of lower M_w. A value of 0.42 was previously found for total Acacia gum (Idris et al., 1998), value also in agreement with a moderately solvent affinity.

As is well-known, molecular parameters and dilute solution properties can be gained from their R_g and R_h values for linear polymers, hyperbranched polymers, dendrimers and dendrimer-like synthetic polymers (Burchard, 1994, 1999). In a given polymer solution, the ratio of geometric to hydrodynamic radius ($\rho = R_g/R_h$) depends on its chain architecture and conformation. The ρ ratio is known to be affected by macromolecular flexibility and polydispersity (Adolphi & Kulicke, 1997). Flexible linear polymers in a good solvent take ρ values in the range 1.5–1.7 and up to >2, whereas the value is 0.778 for a homogeneous sphere (Table 1). Fig. 1d shows the plot of the ρ value vs. M_w. The ρ values were not independent of M_w and ranged from 0.93 to 1.14 (with an average value of 1.035) with increasing M_w. A ρ value of 1.1 was found recently for AGP using asymmetrical flow field-flow fractionation (Alftren, Penarrieta, Bergenståhl, & Nilsson, 2012). The two limiting values of 0.93 and 1.14 were close to the ρ parameter of hyperbranched structures theoretically predicted to be 1.22 (in the Kirkwood approximation for the hydrodynamic interaction) and dendrimer-like synthetic polymers (Gaussian "soft sphere") theoretically predicted to be 0.977 (Burchard, 1999). This would confirm the more globular shape of AGP in the low M_w range while the conformation would expand with increasing M_w. However a ρ value around 1 is also compatible with a two-dimensional object such as an oblate ellipsoid (He & Niemeyer, 2003; Matsuoka et al., 2006). A typical example is amylopectin, a branched polysaccharide from starch, that displays an oblate ellipsoid shape (Lelievre, Lewis, & Marsden, 1986) and a ρ parameter of around 1 (Bello-Pérez, Roger, Colonna, & Paredes-López, 1998). It is also interesting to note that increasing the axial ratio of the ellipsoid, i.e. increasing the axial anisotropy of the particle, promotes an increase in the ρ parameter.

From the average AGP molecular weight M_w of 1.86×10^6 g mol^{-1} and an intrinsic viscosity [η] value of 70.7 mL g^{-1} determined previously (Renard et al., 2006), a hydrodynamic radius R_h value of 27.5 nm was calculated, value slightly lower than the experimental R_h of 34.4 nm determined by dynamic light scattering (Renard et al., 2006). However, the reasonable agreement between the calculated and experimental R_h values revealed that AGP in solution would display on average a globular conformation. Globular and close-packed shape of Acacia gum molecules was suggested previously based on the low viscosity of gum solutions (Anderson & Dea, 1971; Swenson, Kaustinen, Kaustinen, & Thompson, 1968). We will show in the TEM section that a theoretical R_h value of 29 nm can be calculated on the basis of micrographs and the assumption of oblate ellipsoid shapes.

3.2. SANS measurements

Scattering form factor of AGP in D_2O solvent was obtained using SANS. The absence of any correlation peak in the scattering profile demonstrated that 50 mM NaCl was sufficient to suppress intermolecular repulsive interactions (Fig. 2) and confirmed that AGP was a weakly charged polyelectrolyte (Renard et al., 2006). Similar result was obtained by SANS on total Acacia gum (Dror, Cohen, & Yerushalmi-Rozen, 2006).

At low scattering wave vectors q, the scattering function $I(q)$ vs. q followed a power law of the form $I(q) \sim q^{-\alpha}$, with an α value of 1.1. A value of 1 is indicative of a linear conformation typical of a rod or an elongated cylinder (Svergun & Koch, 2003). The AGP radius of gyration (R_g) was however not calculated from the Guinier region as the condition $qR_g < 1$ was not fulfilled in the q range explored. At intermediate scattering wave vectors q, the scattering function also followed a power law with an exponent value α of 2.13. A value of 2 is indicative of the presence of an isolated population of disk-like particles, and more generally of a 2D particles morphology (Svergun & Koch, 2003), or of a fractal structure. From the exponent α, the affinity ν of AGP for the solvent was estimated to be as 0.47 ($\alpha = 1/\nu$), value corresponding to a theta solvent, intermediate between a poor affinity ($\nu = 0.33$) and a very good affinity ($\nu = 0.6$) for the solvent. This finding was in total agreement with the solvent affinity found from ν_h exponents ($M_w < 2 \times 10^6$ g mol^{-1}) using HPSEC coupled to on-line viscosimeter.

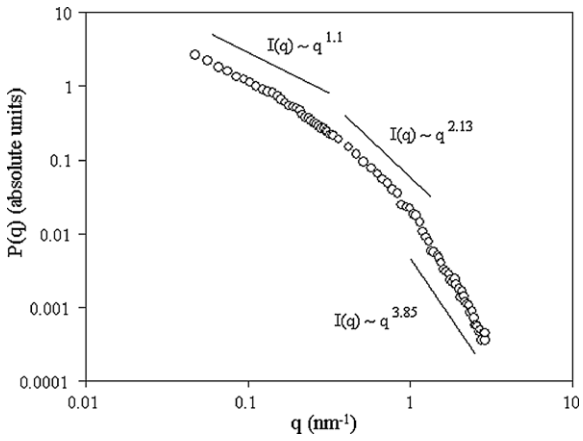

Fig. 2. Form factor of arabinogalactan-protein (AGP) from Acacia gum (1 wt%) obtained at 25 °C in D_2O containing 50 mM NaCl. The exponent of the power law in the low q range (1.1) indicated a linear or elongated conformation. From the exponent of the power law in the intermediate q range, an affinity of AGP for the solvent of 0.47 (1/2.13) can be calculated (theta solvent). The exponent in the high q range indicated a fractal surface structure ($D_f = 2.15$).

In the high q range, where the local structure of scattering objects is probed, scattering intensity followed a power law with an exponent of 3.85. This clearly indicated that AGP had a

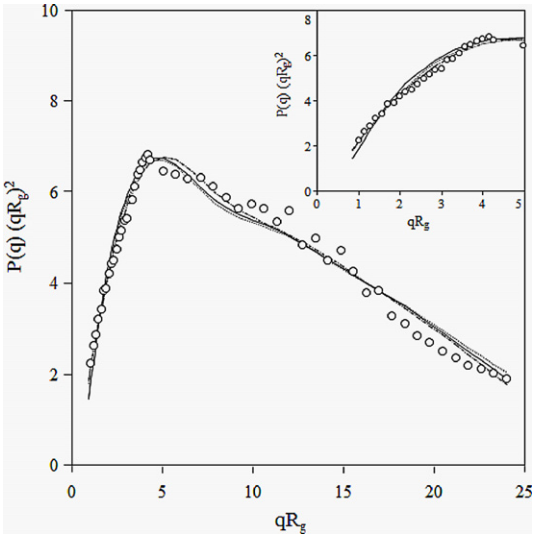

Fig. 3. Kratky-type plot using an affinity for the solvent of 0.5 of scattering curve of AGP from Acacia gum (1 wt%) in D_2O containing 50 mM NaCl and theoretical form factors of triaxial ellipsoids with semi axes 1.2, 9.4 and 32 nm (—) or 1.2, 8.6 and 58 nm (- - - -), or of an elliptical cylinder with 75.4 nm length, 1.25 nm minor semi-axis and a major/minor semi-axis ratio of 7 (.....). Inset: Enlargement of the small qR_g range.

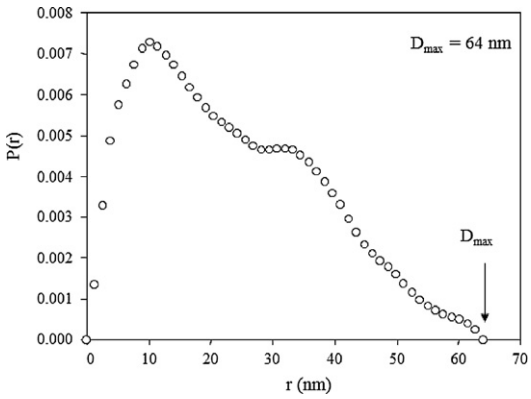

Fig. 4. Pair distance distribution function $P(r)$ calculated by indirect Fourier transform for the arabinogalactan-protein (AGP) from Acacia gum form factor using GNOM software. Maximum dimension of AGP (D_{max}) was 64 nm.

fractal surface structure with a fractal dimension value D_f of 2.15, with exponent = $2d_v - D_f$, d_v and D_f being the contribution of volume and surface dimensions at interfaces between the macromolecule and the solvent.

Since the arabinogalactan-peptide fraction (AG) from Acacia gum was described as a thin oblate ellipsoid (Sanchez et al., 2008), a fit of the AGP form factor using elliptical cylinder (Pedersen, 1997) and oblate ellipsoid theoretical form factor models was attempted taking into account the fact that HPSEC-MALLS revealed conformations between sphere or random coil and more elongated structure and SANS identified a rather elongated conformation and particles with 2D morphologies. Finally, it appeared that a tri-axial ellipsoid form factor (with semi-axes 1.2, 9.4 and 32 nm or 1.2, 8.6 and 58 nm) or an elliptical cylinder (with length of 75.4 nm, minor semi-axis of 1.25 nm and a major/minor semi-axis ratio of 7) reasonably fitted experimental data (Fig. 3). The fit was not completely satisfying, however the overall characteristic of the form factor was approached. It is important to note that the fit was better at small q with longer particle, emphasizing the possible existence of two particle populations as suggested by the R_g vs. M_w relationship (see Fig. 1b). It can be also noted that the two satisfying theoretical form factors suggested a rather "two-dimensional" conformation of AGP, as opposed to a more globular conformation. The possible conformation of AGP can be estimated as a first approximation from the shape of the pair distance distribution function $P(r)$, calculated from the form factor $P(q)$ by indirect Fourier transform. The AGP $P(r)$ function is displayed in Fig. 4. From this function, the maximum distance (D_{max}) found for AGP was of 64 nm. Note that this value was used to fit the experimental form factor by the tri-axial ellipsoid theoretical form factor. The shape of the $P(r)$ function suggested the presence of heterogeneous rather elongated particles with two preferential distances as two maxima were observed (Fig. 4) (Glatter, 1982). The first maximum corresponded to a half-distance of 10 nm and the second one to a half-distance of about 32 nm. Alternatively, the presence of two maxima can also indicate the presence of two particles differing in dimensions.

3.3. Transmission electron microscopy (TEM)

Two TEM micrographs are shown in Fig. 5. These two micrographs were carefully selected and were representative of the 25 pictures we analysed. The first remark is that a distribution of sizes

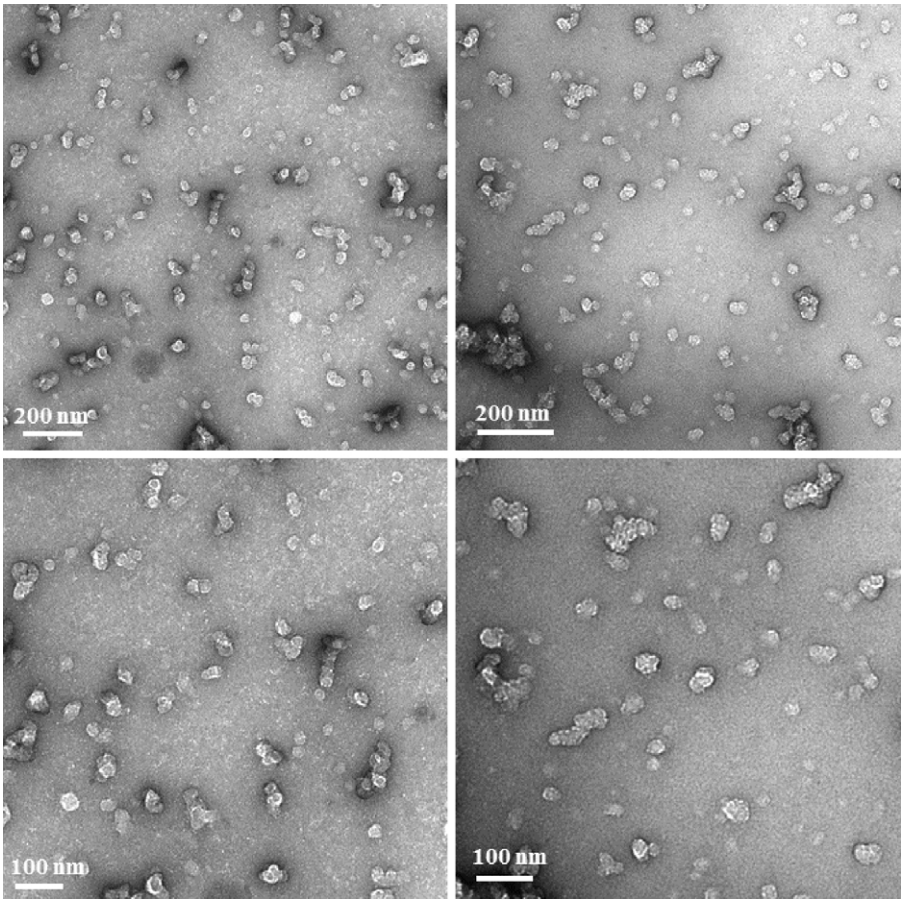

Fig. 5. TEM micrographs at two magnifications of arabinogalactan-protein (AGP) from Acacia gum dispersed at 1 wt% at 25 °C in 50 mM NaCl.

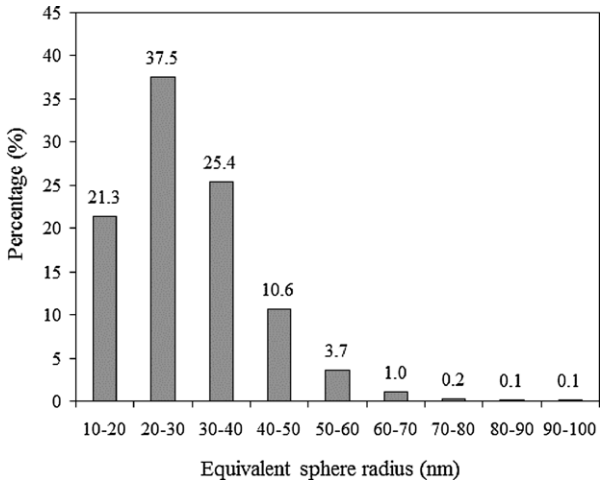

Fig. 6. Size distribution (equivalent sphere radius) of particles from TEM micrographs of arabinogalactan-protein (AGP) from Acacia gum dispersed at 1 wt% in 50 mM NaCl. Raw micrographs were thresholded before surface area of particles were recorded and transformed into equivalent sphere radii. About 5400 particles from 25 distinct micrographs were analysed. All image processing were performed using the ImageJ freeware v1.45o. Percentage *per* size class is indicated above bars.

was clearly apparent. Small particles with apparent diameters of 10–20 nm were present besides larger particles with maximum dimensions of about 100 nm and up to 200 nm. The second important remark is that, while a majority of single particles appeared, aggregated structures were also present. Single particles displayed a more or less anisotropic spheroidal shape but aggregated structures had in general more elongated shapes. In order to have an idea of the size distribution of particles, we computed from micrographs their equivalent sphere radii based on their apparent surface. One could object that such information is of weak value as far as highly anisotropic objects are considered. However, it is important to realize that about 60% of treated particles displayed axial ratios (ratio between minor and major axis of particles) comprised between 1 and 1.4. Our analysis revealed that about 85% of particles displayed an apparent diameter comprised between 20 and 80 nm (Fig. 6), which is roughly compatible with structural dimensions deduced from the $P(r)$ function (see Fig. 4). Only 15% of particles were larger, with apparent diameters comprised between 80 and 120 nm, these particles corresponding mainly to elongated aggregates. From the minor (b) and major (a) axis of analysed particles, and considering that the latter are oblate-type ellipsoids, we can calculate a theoretical R_h value using the equation $[(a^2-b^2)^{1/2}]/\tan^{-1}[((a^2-b^2)/b^2)^{1/2}]$ (He & Niemeyer, 2003). The averaged R_h value we found was 29 nm, a value close to the experimental 34.4 nm value.

The use of uranyl acetate to highlight morphological details of particles induces the appearance of white heterogeneities, suggesting 3D structural heterogeneities. In order to check this assumption, we captured individual (single and moderately assembled) objects from micrographs and made some image analyses. Typical examples of results obtained are shown in Fig. 7, with smaller objects appearing more spherical than larger ones that were somewhat more elongated. However, a remarkable feature of all particle morphologies was the presence of an outer structure combined to an inner more or less porous network of interspersed chains or interacting structural blocks. The same kind of morphology was demonstrated for the arabinogalactan (AG) fraction of Acacia gum (Sanchez et al., 2008). In addition, it is possible that the particle in Fig. 7c could be an assembly of AG. Considering that particles in pictures g, h, j, k and l were assemblies of single particles, all particles displayed structural similarities. However, clear differences were observed in the density and morphology of the inner porous network. Some particles displayed a quite dense inner network (e.g. pictures b, d, g, j, k) while other particles had a more porous one (e.g. pictures a, c, e, f, h, I, l).

The 3D rendering of particles clearly indicated that AGP family from Acacia gum were mostly flat objects with thickness probably below 3–5 nm. In addition, the thickness h of AGP can be roughly estimated from the point where $F(r)$ function (=$P(r)/r$) became linear (data not shown) (Glatter, 1982) and was found to have a value lower than 3 nm. The thickness estimate is in agreement with the smaller dimension values (~2.5 nm) found by fitting SANS experimental form factor.

The micrographs we have described were obtained scanning negative films at low resolution. The main objective was to get a first description of the structural and morphological diversity of AGP and to extract some structural dimensions. In a second step, we scanned negative films at high resolution (about 1 nm for 3 pixels). At this scale, it was possible to observe for the first time the finest details of AGP structure as shown in Fig. 8. It is clear that the high resolution did not change the fact that single objects (Fig. 8a, b, e, and h) coexisted with assembled objects (Fig. 8c, d, f, and g). However, we can now observe in more details that single objects with very similar structural dimensions and morphology can have very different structures. In this light, the comparison of Fig. 8a and b is particularly informative. Fig. 8a closely looks like an AG as those shown previously (Sanchez et al., 2008). Fig. 8b and c could be single AGP. Regarding assemblies, the existence of assembled AG as part of the AGP family is confirmed (Fig. 8d). Fused AGP dimers (Fig. 8c and h), trimers (Fig. 8g) or tetramers (Fig. 8f) were clearly observed as well as multimers, not shown in Fig. 8 but present in Fig. 7. Probably more impressive is the particle-dependent inhomogeneous distribution of 3D structural blocks (along z axis, in white) and porosity.

4. Discussion

The molecular fractions in whole gum are classically denoted AG, AGP and GP in literature even if the great biochemical similarity between the fractions could induce some cross-contaminations during chromatographic separation. This was indeed what we observed in AGP fraction after HIC separation where some AG molecules were also present (see Fig. 5). Our study is however mainly concerned by the so-called AGP component of Acacia gum, which is the second more important fraction, in weight, isolated by HIC. The question of AGP structure from Acacia gum is a matter of debate since more than 50 years. One reason is that AGP are complex macromolecules differing in the sugar and amino acid composition, degree of branching, charge density and shape. From a number of experimental data on total Acacia gum, e.g. the power-law exponents in the $[\eta]$ vs. M_w or R_g vs. M_w relationships, or the low viscosity of gum solutions, globular random coil and close-packed shapes of Acacia gum molecules, including AGP, were suggested. Including the so-called wattle-blossom model (see Section 1), the current hypothesis is that AGP is a spheroidal random coil composed of a folded polypeptide chain carrying large carbohydrate blocks with thin oblate ellipsoid morphologies (Mahendran et al., 2008). More recently, it was suggested that AGP would be in fact a molecular association resulting from an aggregated fraction of AG units stabilized by low molecular weight proteinaceous components found in the glycoprotein (GP) fraction of Acacia gum (Al-Assaf, Sakata, McKenna, Aoki, & Phillips, 2009). The main objective of the present study was to probe these different hypotheses and to provide if possible a clearer view of AGP structure, combining SEC-MALLS measurements, SANS and TEM.

SEC-MALLS measurements clearly indicated that AGP was composed of macromolecules differing in shape according to their

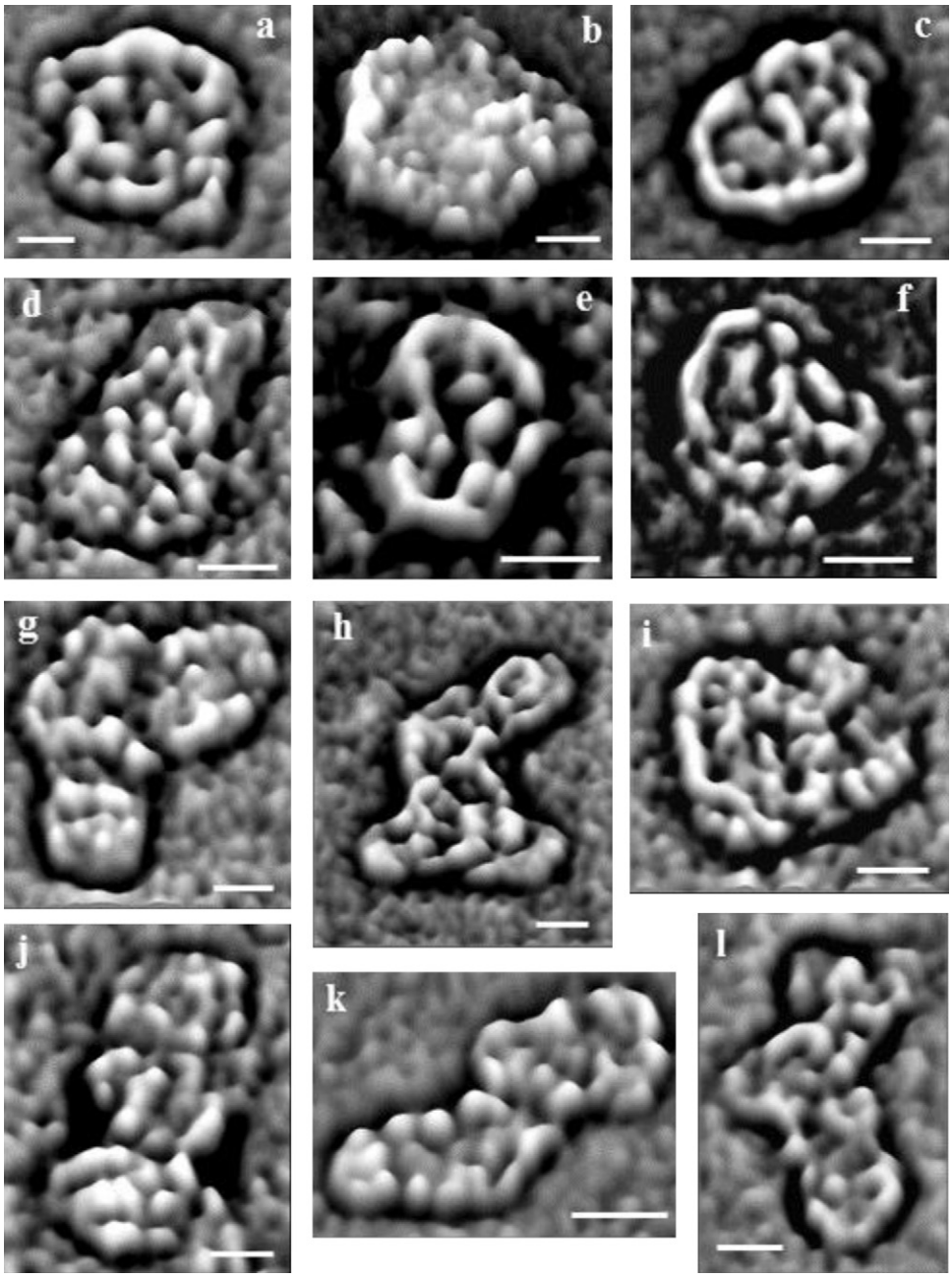

Fig. 7. Structural details of twelve particles (a–l) captured from TEM micrographs of arabinogalactan-protein (AGP) from Acacia gum dispersed at 1 wt% in 50 mM NaCl. After capturing one particle from raw micrographs such as those shown in Fig. 5, image contrast was changed and images were filtered using a bandpass FFT filter then (in some cases) using the CLAE (Contrast Limited Adaptive Histogram Equalization) ImageJ plugin. After filtering, 3D rendering was applied through the Interactive 3D Surface Plot v2.33 plugin. All scale bars indicates 20 nm.

molar masses. The low molar mass population would be rather globular while the high molar mass population would be rather elongated. These hypotheses were confirmed by the fractal dimension values determined from the exponents of $R_g - M_w$ and $[\eta] - M_w$ relationships where $d_f = 1/\nu_g$ and $d_f = 3/1 + \alpha$, respectively. d_f values of 2.4 and 2.2 were found for the low molar mass population while d_f values of 1.1 and 1.6 were found for the high molar mass population, highlighting again the more extended conformation of AGP macromolecules in the high M_w range. The low fractal dimension values found for the high molar mass population were in very good agreement with the 1.1 value identified by SANS for the dependence of scattering intensity at low q values. The presence of two macromolecular populations differing in length can partly explain the existence of two maxima in the pair distance distribution function calculated from the averaged form factor recorded by SANS (see Fig. 4). This can also account for the better fit of form factor at small q using longer molecules (see Fig. 3).

A first hypothesis is that the two AGP conformations are caused by heterogeneity in the degree of branching. AGP is known to be a (hyper)-branched polysaccharide for which the variation in the degree of branching could reflect the asymmetric molecular weight distribution identified in Fig. 1a. The diversity of conformations would thus be reflected through the two exponent values identified in the R_g, $[\eta]$, R_h and ρ vs. M_w relationships, probably highlighting the variability of branching and therefore conformations in AGP macromolecules. AGP in solution would behave as a branched or hyper-branched glycopolymer with conformations ranging from globular to elongated shape depending on

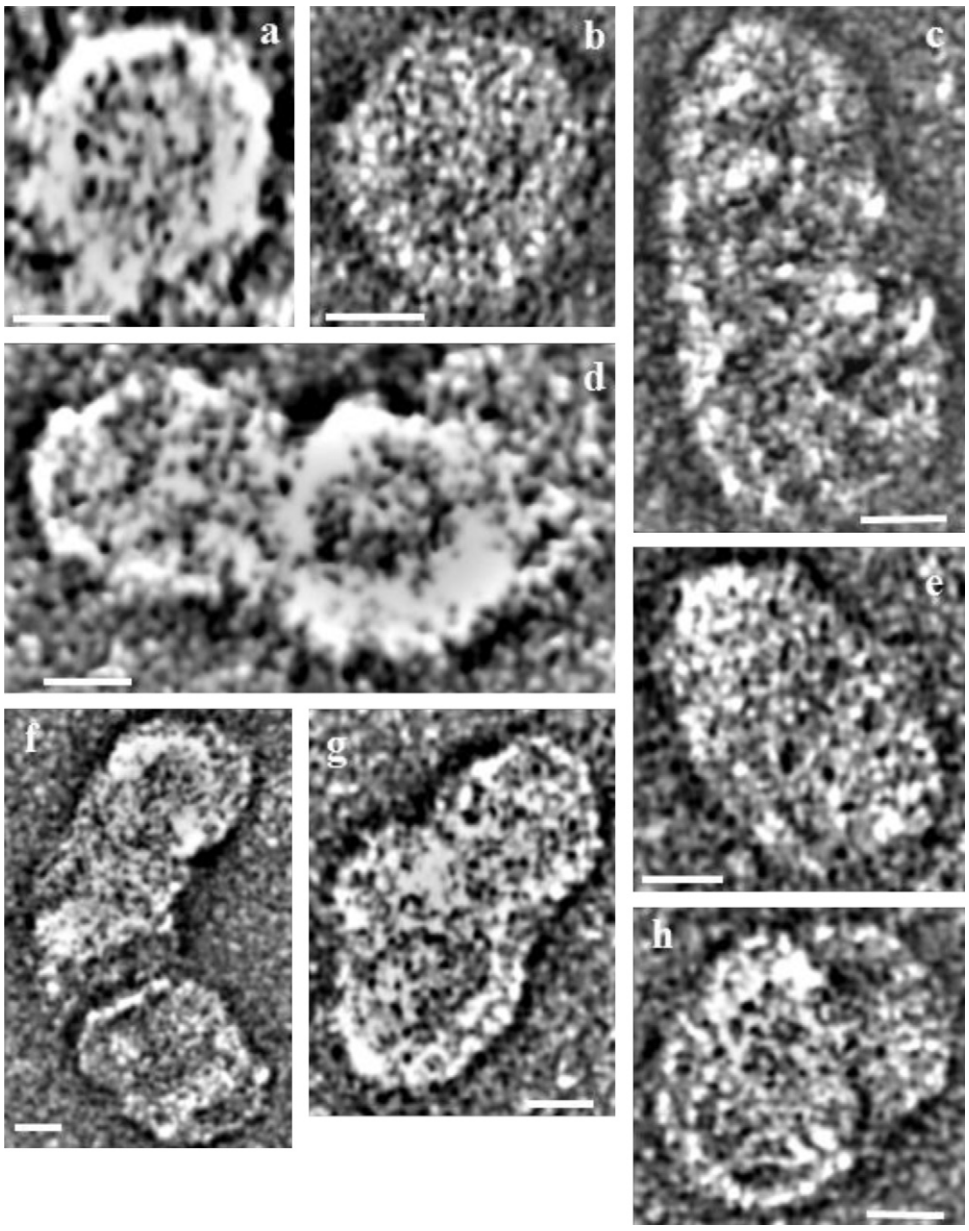

Fig. 8. Structural details at high resolution of eight particles (a–h) captured from TEM micrographs of arabinogalactan-protein (AGP) from Acacia gum dispersed at 1 wt% in 50 mM NaCl. After capturing one particle from raw micrographs, image contrast was changed and images were filtered using a bandpass FFT filter then (in some cases) using the CLAE (Contrast Limited Adaptive Histogram Equalization) ImageJ plugin. All scale bars indicates 20 nm.

the size of the AGP branches. This partial conformational analysis would reflect the relative large size polydispersity of side chains (oligosaccharidic side chains and polysaccharidic blocks of different length and density of branching) generally described in literature for AGP macromolecules (Pettolino et al., 2006). Indeed, our findings regarding the increase of ν_g and ν_h exponent values with increasing molecular weight M_w would mean that the low molar mass population ($1–2 \times 10^6$ g mol^{-1}) would be denser than the high molar mass population. Deviation of the molar mass dependence of R_g and therefore ν_g exponent for high molar mass would be clearly indicative of short-chain branching (Rolland-Sabaté, Mendez-Montealvo, Colonna, & Planchot, 2008). In addition, the ρ-parameters calculated for AGP and found to be between 0.93 and 1.14 (Fig. 1d) were close to the theoretical value predicted by the theory of hyperbranched polymers according to the Kirkwood–Riseman approximation for hydrodynamic interaction (~1.225) (Burchard, 1999). However, as the Kirkwood–Riseman approximation underestimates the effect of the hydrodynamic interaction, the asymptotic limit could thus be reduced to 1.09–0.98 (Ioan, Aberle, & Burchard, 2000). These values were consistent with the experimental results of the present study.

The main preliminary conclusions coming from HPSEC-MALLS analyses were thus that the low molar mass population had long-chain branching inducing an increase of macromolecule apparent density while the invert applied for the high molar mass population, i.e. short-chain branching and decrease of apparent density (apparent density was calculated according to the relation $d_{app} = M_w/N_a(4\pi/3)R_g^3$, data not shown).

These conclusions are based on the hypothesis that AGP are isolated molecules and that their conformation is only determined by their degree of branching and, possibly, their affinity for the solvent. An additional hypothesis, that is not exclusive from the first one, is that high molar mass elongated AGP are not single molecules but molecular assemblies. Only one study using TEM highlighted an

extended architecture with an ellipsoidal structure for an AGP with dimensions of 15 nm × 25 nm for the minor and major axes, respectively (Baldwin, McCann, & Roberts, 1993). It was observed in this study that AGP macromolecules also displayed a higher contrast in the outer part of ellipsoids compare to the inner part, revealing a structural inhomogeneity. The discovery of an ellipsoidal structure was interpreted as an indication of the reliability of the wattle blossom model for AGP. In a more recent study, spheroidal micelles-like aggregates with diameters of around 20 nm were seen by cryo-TEM in total Acacia gum (Dror et al., 2006). However, the authors also attributed these structures to the larger component of the gum, i.e. AGP.

Our TEM observations on AGP revealed for the first time the existence of two types of conformations, anisotropic spheroidal shape with an average diameter of 50–70 nm and more elongated shape that could be ascribed to the association of structural blocks with minor and major axes of, respectively, 20–30 and 80–100 nm. The molecular associations of structural blocks could come from the flexibility of the AGP as revealed in Fig. 3 where the Kratky-type representation clearly displayed a scattering behaviour of anisotropic particles with some degree of flexibility. In addition, even if structural similarities were observed on both conformations, clear differences were noticed in the density and morphology of the inner porous network. As well, particles with similar whole morphologies and sizes can have different chain densities and shapes. These observations were in agreement with the two conformations identified by HPSEC-MALLS and would reflect again the large size polydispersity of the oligo and (poly)-saccharidic blocks attached to the polypeptidic backbone. Another important insight from TEM observations is that isolated AGP apparently do not display globular closed-packed random coil conformations. AGP from Acacia gum are indeed two-dimensional highly porous network of interspersed chains and interacting carbohydrate blocks. It can be inferred that the two-dimensional appearance of AGP is just a consequence of sample preparation for TEM, indeed one can imagine that a flexible globular 3D particle could appear as ellipsoidal upon adsorption onto the carbon-coated grid. However, both the power-law exponent (2.13) obtained in the intermediate q range of the SANS form factor and the best fit by theoretical form factors suggested a two-dimensional morphology for AGP. The 2D morphology highlighted the great steric constraints imposed by the spatial arrangement of polysaccharidic moieties along the polypeptidic backbone. The recent compact globular model proposed for AGP is interesting but do not consider these geometrical constraints (Mahendran et al., 2008). In particular, the random coil conformation depicted for the polypeptidic backbone in the new model was in contradiction with the presence of secondary structures, in particular PPII-helices and β-strands, we identified by circular dichroism (Renard et al., 2006). Finally, the flat characteristic of AGP, combined to its intrinsic flexibility and porous structure likely contribute to the unusual low viscosity of Acacia gum dispersions and its hydration properties. Table 2 summarizes the main structural parameters determined in this study for the individual arabinogalactan-protein (AGP) from Acacia gum.

TEM observations clearly indicated that elongated particles also appeared following the molecular assembly of individual AGP (Figs. 7g, h, j, k, l and 8c, d, f, g, h). We cannot exclude that part of aggregated AGP structures were induced by sample preparation for microscopy, especially during the dehydration step. Such assemblies are intrinsic structural characteristics of what is called AGP, as suggested by Aoki, Al-Assaf, Katayama, and Phillips (2007) and Al-Assaf et al. (2009). The driving force of the molecular associations would be driven by polypeptidic backbone interactions, probably through hydrophobic associations, and maybe intermolecular disulphide bonds as free cysteine residues were identified in AG and GP molecular fractions from Acacia gum (Renard et al., 2006).

Table 2
Summary of arabinogalactan-protein (AGP) from Acacia gum structural parameters determined by SANS, HPSEC-MALLS and the pycnometric method, or calculated.

Structural parameters	Values
M_w (g mol^{-1})	1.86×10^6
M_w/M_n	1.33
D_{max} (nm)	64
R_g (nm)	30[a]
R_h (nm)	27.5,[b] 34.4[c]
Translational diffusion coefficient D (10^7 cm^2 s^{-1})	0.63
$[\eta]$ (mL g^{-1})	70.7
Density	1.005[d]
Partial specific volume (mL g^{-1})	0.995
Specific volume (mL g^{-1})	6
Hydration parameter δ (g g^{-1})	5[e]
Hydrated volume (mL)	18.6×10^{-18}
Flory–Fox parameter Φ	12.6×10^{23}[f]
Solvent affinity	0.4[g]
Fractal dimension D_f	2.1,[h] 2.4,[i] 2.2[j]
Scattering length density (cm^{-2})	2.81×10^{10}[k]

[a] From HPSEC-MALLS.
[b] Calculated from the equation $[\eta] = 6.308 \times 10^{24} R_h^3/M_w$ (32).
[c] Determined by dynamic light scattering at three scattering angles (30°, 90° and 150°).
[d] A value of 1.003 was found for total Acacia gum (41). Please note that the same value was found for Acacia gum by pycnometry.
[e] Taken from Takigami, Takigami, and Phillips (1995).
[f] From the Flory–Fox equation $\Phi = 4.291 \times 10^{21}(R_h/R_g)^3$.
[g] (1/2.13) power law in the intermediate q range of $P(q)$.
[h] Determined in the intermediate q range from the power law $I(q) \sim q^{-D_f}$.
[i] Determined from $R_g = KM_w^{\nu}$ in the low M_w range with $d_f = 1/\nu_g$.
[j] Determined from $[\eta] = KM_w^{\alpha}$ in the low M_w range with $d_f = 3/1 + \alpha$.
[k] Calculated from contrast variation measurements (matching AGP scattering intensity for D_2O 48.1% in 23 mM NaCl).

Finally, the hypothesis that AGP could be an aggregated fraction made up of AG units stabilized by low molecular weight highly proteinaceous components (i.e. GP fraction) was examined (Al-Assaf et al., 2009; Aoki et al., 2007). More accurately, maturation process would promote interactions between AGP, AG and GP, inducing a molecular reorganization of the system and the appearance of composite AGP architectures. In addition, spray-drying was found to increase the molecular weight of the AGP fraction due to AGP aggregation (Al-Assaf, Andres-Brull, Cirre, & Phillips, 2012). These findings were in particular reinforced by the fact that the number of amino acid residues we calculated for the AGP fraction was very high (i.e. 2253 amino acid residues) and that several glycoproteins domains, maybe linked by intermolecular disulphide bonds, could account for this abnormal high value (Renard et al., 2006). TEM observations are not sufficiently discriminatory but it seems that in our AGP sample, aggregated AG and aggregated AGP make a significant contribution to the whole aggregated AGP population. This aggregation would occur during drying process of Acacia gum but also could be induced by biological factors such as location or age of the tree. Main factors affecting aggregation could come from intermolecular H-bonds between the saccharidic moieties as suggested by Mahendran et al. (2008) and/or polypeptidic backbone interactions through hydrophobic interactions and intermolecular disulphide bonds.

5. Conclusion

Arabinogalactan-protein (AGP) from Acacia gum was found to be constituted of two populations, a low molar mass population with long-chain branching and globular shape and a high molar mass population with short-chain branching and elongated shape. AGP would behave in solution as a branched or hyper-branched polymer with conformations ranging from globular to elongated shape depending on the size of the carbohydrate branches. Small angle neutron scattering (SANS) further revealed that the

maximum AGP dimension was of 64 nm and that a tri-axial ellipsoid with semi-axes values of 9.4, 32 and 1.2 nm of thickness reasonably fitted the data. Transmission electron microscopy (TEM) highlighted the existence of two types of flat objects with thicknesses below 3–5 nm, single particles with a more or less anisotropic spheroidal shape and aggregated structures with a more elongated shape, in agreement with HPSEC-MALLS data. A remarkable feature of all particle morphologies was the presence of an outer structure combined to an inner more or less porous network of interspersed chains or interacting structural blocks, as previously found for the arabinogalactan (AG) main molecular fraction of Acacia gum. However, clear differences were observed in the density and morphology of the inner porous network, probably highlighting differences in the degree of branching. The aggregated structures we identified by TEM would reinforce the recent hypothesis that, upon maturation, interactions between the different starting molecular fractions of Acacia gum, i.e. AG, AGP and GP as obtained by HIC, induce the formation of high molar mass composite supramolecular architectures. Thus, the so called AGP, is in fact a heterogeneous population varying in anisotropy, chain density and porosity, and of all possible molecular combinations between AG, AGP and GP. This structural heterogeneity likely depends on chemical composition of gum sample and its maturation process, natural or induced by processing. Functional properties of AGP are supposed to be strongly dependent on the relative proportion of the different macromolecular and supramolecular species. This could partly explain the different functional properties, for instance surface properties, observed for Acacia gum samples containing the same percentage in AGP.

Acknowledgements

We would like to acknowledge L. Lavenant-Gourgeon for AGP purification, M.-J. Crepeau and M.-C. Ralet for HPSEC-MALLS measurements and data treatments, and E. Lepvrier for TEM observations.

References

Adolphi, U., & Kulicke, W.-M. (1997). Coil dimensions and conformation of macromolecules in aqueous media from flow field-flow fractionation/multi-angle laser light scattering illustrated by studies on pullulan. *Polymer*, *38*, 1513–1519.

Al-Assaf, S., Sakata, M., McKenna, C., Aoki, H., & Phillips, G. O. (2009). Molecular associations in acacia gums. *Structural Chemistry*, *20*, 325–336.

Al-Assaf, S., Andres-Brull, M., Cirre, J., & Phillips, G. O. (2012). Structural changes following industrial processing of Acacia gums. In J. F. Kennedy, G. O. Phillips, & P. A. Williams (Eds.), *Gum Arabic* (pp. 153–168). London: The Royal Society of Chemistry.

Alftren, J., Penarrieta, J. M., Bergenståhl, B., & Nilsson, L. (2012). Comparison of molecular and emulsifying properties of gum Arabic and mesquite gum using asymmetrical flow field-flow fractionation. *Food Hydrocolloids*, *26*, 54–62.

Anderson, D. M. W., Bridgeman, M. M. E., Farquhar, J. G. K., & McNab, C. G. A. (1983). The chemical characterization of the test article used in toxicological studies of gum Arabic (*Acacia senegal* (L.) Willd). *International Tree Crops Journal*, *2*, 245–254.

Anderson, D. M. W., & Dea, I. C. M. (1971). Recent advances in the chemistry of Acacia gums. *Journal of Society of Cosmetic Chemistry*, *22*, 61–76.

Anderson, D. M. W., & Stoddart, J. F. (1966). Studies on uronic acid materials. *Carbohydrate Research*, *2*, 104–114.

Aoki, H., Al-Assaf, S., Katayama, T., & Phillips, G. O. (2007). Characterization and properties of *Acacia senegal* (L.) Willd. var. senegal with enhanced properties (Acacia (sen) SUPER GUM TM): Part 2—Mechanism of the maturation process. *Food Hydrocolloids*, *21*, 329–337.

Baldwin, T. C., McCann, M. C., & Roberts, K. (1993). A novel hydroxyproline-deficient arabinogalactan protein secreted by suspension-cultured cells of *Daucus carota* (purification and partial characterization). *Plant Physiology*, *103*, 115–123.

Bello-Pérez, L. A., Roger, P., Colonna, P., & Paredes-López, O. (1998). Laser light scattering of high amylose and high amylopectin materials, stability in water after microwave dispersion. *Carbohydrate Polymers*, *37*, 383–394.

Burchard, W. (1994). Light scattering. In S. B. Ross-Murphy (Ed.), *Physical techniques for the study of food biopolymers* (pp. 343–392). London: Blackie Academic & Professional.

Burchard, W. (1999). Solution properties of branched macromolecules. *Advances in Polymer Science*, *143*, 113–194.

Carpita, N. (1982). Limiting diameters of pores and the surface structure of plant cell walls. *Science*, *218*, 813–814.

Chevalier, A. (1924). Sur la production de la gomme arabique en Afrique Occidentale. *Revue de Botanique Appliquée & d'Agriculture Coloniale*, *4*, 256–263.

Churms, S. C., Merrifield, E. H., & Stephen, A. M. (1983). Some new aspects of the molecular structure of *Acacia senegal* gum (gum Arabic). *Carbohydrate Research*, *123*, 267–279.

Dror, Y., Cohen, Y., & Yerushalmi-Rozen, R. (2006). Structure of gum Arabic in aqueous solutions. *Journal of Polymer Science Part B: Polymer Physics*, *44*, 2365–3271.

Fincher, G. B., Stone, B. A., & Clarke, A. E. (1983). Arabinogalactan-proteins: Structure, biosynthesis and function. *Annual Review of Plant Physiology*, *34*, 47–70.

Glatter, O. (1982). Interpretation. In O. Glatter, & O. Kratky (Eds.), *Small angle X-ray scattering* (pp. 167–196). London: Academic Press Inc.

He, L., & Niemeyer, B. (2003). A novel correlation for protein diffusion coefficients based on molecular weight and radius of gyration. *Biotechnological Progress*, *19*, 544–548.

Idris, O. H. M., Williams, P. A., & Phillips, G. O. (1998). Characterisation of gum from *Acacia senegal* trees of different age and location using multidetection gel permeation chromatography. *Food Hydrocolloids*, *12*, 379–388.

Ioan, C. E., Aberle, T., & Burchard, W. (2000). Structure properties of dextran. 2. Dilute solution. *Macromolecules*, *33*, 5730–5739.

Kawahigashi, M., Sumida, H., & Yamamoto, K. (2005). Size and shape of soil humic acids estimated by viscosity and molecular weight. *Journal of Colloid and Interface Science*, *284*, 463–469.

Lelievre, J., Lewis, J. A., & Marsden, K. (1986). The size and shape of amylopectin: A study using analytical ultracentrifugation. *Carbohydrate Research*, *153*, 195–203.

Mahendran, T., Williams, P. A., Phillips, G. O., Al-Assaf, S., & Baldwin, T. C. (2008). New insights into the structural characteristics of the arabinogalactan-protein (AGP) fraction of gum Arabic. *Journal of Agricultural and Food Chemistry*, *56*, 9569–9576.

Majewska-Sawka, A., & Nothnagel, E. A. (2000). The multiple roles of arabinogalactan proteins in plant development. *Plant Physiology*, *122*, 3–9.

Matsuoka, K., Yonekawa, A., Ishii, M., Honda, C., Endo, K., Moroi, Y., et al. (2006). Micellar size, shape and counterion binding of N-(1,1-dihydroperfluoroalkyl)-N,N,N-trimethylammonium chloride in aqueous solutions. *Colloid Polymer Science*, *285*, 323–330.

Pedersen, J. S. (1997). Analysis of small-angle scattering data from colloids and polymer solutions: Modelling and least-squares fitting. *Advances in Colloid and Interface Science*, *70*, 171–210.

Pettolino, F., Liao, M. L., Ying, Z., Mau, S. L., & Bacic, A. (2006). Structure, function and cloning of arabinogalactan-proteins (AGPs): An overview. *Food and Food Ingredients Journal of Japan*, *211*, 12–25.

Qi, W., Fong, C., & Lamport, D. T. A. (1991). Gum Arabic glycoprotein is a twisted hairy rope. A new model based on O-galactosylhydroxyproline as the polysaccharide attachment site. *Plant Physiology*, *96*, 848–855.

Randall, R. C., Phillips, G. O., & Williams, P. A. (1989). Fractionation and characterization of gum from *Acacia senegal*. *Food Hydrocolloids*, *3*, 65–75.

Renard, D., Lavenant-Gourgeon, L., Ralet, M.-C., & Sanchez, C. (2006). *Acacia senegal* gum: Continuum of molecular species differing by their protein to sugar ratio, molecular weight, and charges. *Biomacromolecules*, *7*, 2637–2649.

Rolland-Sabaté, A., Mendez-Montealvo, M. G., Colonna, P., & Planchot, V. (2008). Online determination of structural properties and observation of deviations from power law behavior. *Biomacromolecules*, *9*, 1719–1730.

Ross-Murphy, S. B. (1994). Rheological methods. In S. B. Ross-Murphy (Ed.), *Physical techniques for the study of food biopolymers* (pp. 343–392). London: Blackie Academic & Professional.

Sanchez, C., Renard, D., Robert, P., Schmitt, C., & Lefebvre, J. (2002). Structure and rheological properties of acacia gum dispersions. *Food Hydrocolloids*, *16*, 257–267.

Sanchez, C., Schmitt, C., Kolodziejczyk, E., Lapp, A., Gaillard, C., & Renard, D. (2008). The acacia gum arabinogalactan fraction is a thin oblate ellipsoid: A new model based on small-angle neutron scattering and ab initio calculation. *Biophysical Journal*, *94*, 629–639.

Shen, Q., Mu, D., Yu, L.-W., & Chen, L. (2004). A simplified approach for evaluation of the polarity parameters for polymer using the K coefficient of the Mark–Houwink–Sakurada equation. *Journal of Colloid and Interface Science*, *275*, 30–34.

Štepánek, P. (1993). Data analysis in dynamic light scattering. In W. Brown (Ed.), *Dynamic light scattering. The methods and some applications* (pp. 177–241). Oxford: Clarendon Press.

Svergun, D. I. (1992). Determination of the regularization parameter in indirect-transform methods using perceptual criteria. *Journal of Applied Crystallography*, *25*, 495–503.

Svergun, D. I., & Koch, M. H. J. (2003). Small-angle scattering studies of biological macromolecules in solution. *Reports on Progress in Physics*, *66*, 1735–1782.

Svergun, D. I., Semenyuk, A. V., & Feigin, L. A. (1988). Small-angle-scattering-data treatment by the regularization method. *Acta Crystallographica*, *A44*, 244–250.

Swenson, H. A., Kaustinen, H. M., Kaustinen, O. A., & Thompson, N. S. (1968). Structure of gum Arabic and its configuration in solution. *Journal of Polymer Science Part A-2*, *6*, 1593–1606.

Takigami, S., Takigami, M., & Phillips, G. O. (1995). Effect of preparation method on the hydration characteristics of hylan and comparison with another highly cross-linked polysaccharide, gum Arabic. *Carbohydrate Polymers*, *26*, 11–18.

Tanford, C. (1961). Transport processes—Viscosity. In C. Tanford (Ed.), *Physical chemistry of macromolecules* (pp. 317–456). New York: John Wiley & Sons Inc.